Artificial light harvesting by dimerized Möbius ring

Lei Xu (徐磊)
Beijing Computational Science Research Center, Beijing 100084, China

Z. R. Gong (龚志瑞)
School of Physical Sciences and Technology, Shenzhen University, Shenzhen 518060, China

Ming-Jie Tao (陶明杰) and Qing Ai (艾清)*
Department of Physics, Applied Optics Beijing Area Major Laboratory, Beijing Normal University, Beijing 100875, China

(Received 27 June 2017; published 17 April 2018)

We theoretically study artificial light harvesting by a Möbius ring. When the donors in the ring are dimerized, the energies of the donor ring are split into two subbands. Because of the nontrivial Möbius boundary condition, both the photon and acceptor are coupled to all collective-excitation modes in the donor ring. Therefore, the quantum dynamics in the light harvesting is subtly influenced by dimerization in the Möbius ring. It is discovered that energy transfer is more efficient in a dimerized ring than that in an equally spaced ring. This discovery is also confirmed by a calculation with the perturbation theory, which is equivalent to the Wigner-Weisskopf approximation. Our findings may be beneficial to the optimal design of artificial light harvesting.

DOI: 10.1103/PhysRevE.97.042124

I. INTRODUCTION

Photosynthesis is the main resource of the energy supply for living beings on earth. Therein, an efficient light-harvesting process, which delivers the captured photon energy to the reaction center, plays a crucial role in natural photosynthesis [1–4]. Because a series of experimental and theoretical explorations [5–9] have demonstrated that quantum coherent phenomena might exist and even optimize natural photosynthesis, much effort has been made to reveal the effects of quantum coherence on efficient light harvesting [10–17].

Research on the optimal geometries for efficient energy transfer is rare [12,18–21]. Wu *et al.* demonstrated a trapping-free mechanism for efficient light harvesting in a starlike artificial system [18]. Hoyer *et al.* showed a ratchet effect for quantum coherent energy transfer in a one-dimensional system [19]. In 2013, one of the authors (Q.A.) and his collaborators elucidated that clustered geometries utilize exciton delocalization and an energy matching condition to optimize energy transfer in a generic tetramer model [12] as well as in a Fenna-Matthews-Olson complex [22,23]. The quantum dynamics was recently experimentally simulated in nuclear magnetic resonance [24]. However, photosynthesis with a ring-shaped geometry is more frequently observed in natural photosynthetic complexes, e.g., light-harvesting complexes LH1 and LH2 [10,25,26]. This observation inspired Yang *et al.* to prove that symmetry breaking in a B850 ring of a LH2 complex boosts efficient intercomplex energy transfer [20]. Dong *et al.* further proposed that a perfect donor ring for artificial light harvesting makes full use of collective-excitation modes and dark states to enhance energy transfer efficiency [21,27].

Mathematically speaking, the rings as in LH1 and LH2 are topologically trivial, since both the photon and acceptor are only coupled to the zero-momentum collective-excitation mode regardless of the dimerization, as shown in Appendix B. On the other hand, Möbius strips [28–31] manifest novel physical properties and can be used to fabricate novel devices and materials [32], e.g., topological insulators and negative-index metamaterials [33–35]. In these Möbius strips, the electrons in the ring experience different local effective fields at different positions due to a topologically nontrivial boundary condition. This observation enlightens us on the investigation of Möbius strips in artificial light harvesting. When the donors in the ring are dimerized, there are two energy subbands for collective-excitation modes. Due to the Möbius boundary condition, both the photon and acceptor interact with all collective excitations in the ring. This is in remarkable contrast to the case in Ref. [21], where they are only coupled to a single collective-excitation mode.

This paper is organized as follows: The donor ring with a Möbius boundary condition is introduced for light harvesting in the next section. Then, in Sec. III, energy transfer efficiency is numerically simulated for various parameter regimes. In Sec. IV, a possible realization of a dimerized ring with a Möbius boundary condition is given. Finally, the main results are summarized in the Conclusion section. In Appendix A, a brief description of diagonalizing a dimerized ring with a Möbius boundary condition is given. In Appendix B, we prove that both the photon and acceptor only interact with one of the collective-excitation modes in the ring with a periodical boundary condition, regardless of whether or not dimerization exists. In Appendix C, we present a detailed perturbation theory for describing the energy transfer in a ring with a Möbius boundary condition.

*aiqing@bnu.edu.cn

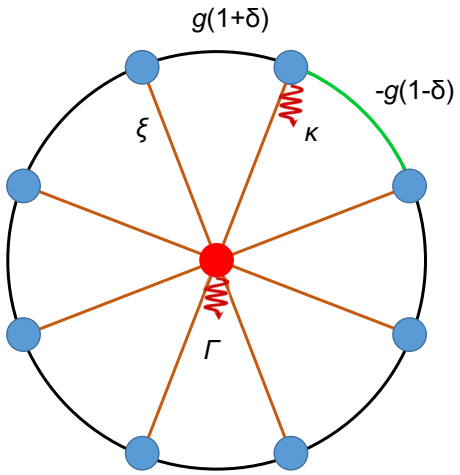

FIG. 1. Schematic of light harvesting by a dimerized ring with a Möbius boundary condition. N donors form a dimerized ring with equal site energy. The green curve on the ring labels the Möbius boundary condition. Due to dimerization, there are two different kinds of alternative couplings between nearest neighbors, i.e., $g(1 \pm \delta)$. An acceptor is located in the center of the ring with site energy ε_A. All donors are uniformly coupled to the acceptor with strength ξ. The fluorescence rate of the donor is κ, while the charge-separation rate on the acceptor is Γ.

II. DIMERIZED RING WITH MÖBIUS BOUNDARY CONDITION

In this paper, we consider light harvesting in a Peierls distorted chain with a Möbius boundary condition (see Fig. 1) [36,37]. The quantum dynamics of the whole system is governed by the Hamiltonian

$$H = \omega b^\dagger b + \varepsilon_A A^\dagger A + H_{\rm PM} + \sum_{j=1}^{N} d_j^\dagger(\xi A + J b) + {\rm H.c.}, \tag{1}$$

where $b^\dagger$ (b) is the creation (annihilation) operator of a photon with frequency ω, $A^\dagger$ (A) is the creation (annihilation) operator of an excitation at the acceptor with site energy ε_A, $d_j^\dagger$ (d_j) is the creation (annihilation) operator of an excitation at the jth donor, and the Peierls distorted ring with a Möbius boundary condition is described by

$$\begin{aligned} H_{\rm PM} = &\sum_{j=1}^{N-1} g[1-(-1)^j\delta] d_{j+1}^\dagger d_j \\ &- g[1-(-1)^N\delta] d_1^\dagger d_N + {\rm H.c.}, \end{aligned} \tag{2}$$

with g being the coupling constant between nearest neighbors and δ being the dimerization constant. Notice that the minus sign before the second term on the right-hand side indicates the Möbius boundary condition [37], and the site energies of donors are homogeneous and chosen as the zero point of energy. Here, we assume that the photon and acceptor are coupled to all donors with equal coupling strengths J and ξ, respectively.

By the diagonalization method of $H_{\rm PM}$ in Appendix A, the total Hamiltonian is rewritten as

$$H = \omega b^\dagger b + \varepsilon_A A^\dagger A + \sum_k \varepsilon_k (A_k^\dagger A_k - B_k^\dagger B_k) + H_1. \tag{3}$$

There are two energy subbands in the donor ring denoted by the annihilation (creation) operators,

$$A_k = \sum_{j=1}^{N/2} \frac{e^{-ikj}}{\sqrt{N}} \left[e^{i(2j-1)\frac{\pi}{N}} d_{2j-1} + e^{i\left(\theta_k + 2j\frac{\pi}{N}\right)} d_{2j} \right], \tag{4}$$

$$B_k = \sum_{j=1}^{N/2} \frac{e^{-ikj}}{\sqrt{N}} \left[e^{i(2j-1)\frac{\pi}{N}} d_{2j-1} - e^{i\left(\theta_k + 2j\frac{\pi}{N}\right)} d_{2j} \right] \tag{5}$$

($A_k^\dagger$ and $B_k^\dagger$) with the eigenenergies being $\pm\varepsilon_k$, where

$$\varepsilon_k = 2g\sqrt{\cos^2\left(\frac{k}{2}-\frac{\pi}{N}\right) + \delta^2 \sin^2\left(\frac{k}{2}-\frac{\pi}{N}\right)}, \tag{6}$$

and the momentum

$$k = \frac{4\pi}{N}\left(0,1,2,\ldots,\frac{N}{2}-1\right) - \pi + \frac{2\pi}{N}. \tag{7}$$

The interaction Hamiltonian among the photon and acceptor and donor ring is

$$\begin{aligned} H_1 &= \sum_k (\xi_{Ak} A_k^\dagger + \xi_{Bk} B_k^\dagger) A + (J_{Ak} A_k^\dagger + J_{Bk} B_k^\dagger) b + {\rm H.c.}, \\ &= \sum_k (h_{Ak} A_k^\dagger + h_{Bk} B_k^\dagger)(\xi A + J b) + {\rm H.c.}, \end{aligned} \tag{8}$$

with the k-dependent factors

$$h_{Ak} = \frac{1}{\sqrt{N}} \sum_{j=1}^{N/2} e^{-ikj} e^{-i(2j-1)\frac{\pi}{N}} (1 + e^{i\theta_k} e^{i\frac{\pi}{N}}), \tag{9}$$

$$h_{Bk} = \frac{1}{\sqrt{N}} \sum_{j=1}^{N/2} e^{-ikj} e^{-i(2j-1)\frac{\pi}{N}} (1 - e^{i\theta_k} e^{i\frac{\pi}{N}}), \tag{10}$$

$$e^{i\theta_k} = \frac{g}{\varepsilon_k}[(1+\delta)e^{-i\frac{\pi}{N}} + (1-\delta)e^{-i\left(k-\frac{\pi}{N}\right)}]. \tag{11}$$

Before investigating the quantum dynamics of light harvesting, we shall analyze the energy spectrum of the Möbius ring for different dimerizations δ. As shown in Fig. 2, the characteristics of the energy spectrum vary remarkably in response to the change of δ. When the donors in the ring are equally distributed, i.e., $\delta = 0$, the energy spectrum $\varepsilon_k = 2g\cos(k/2)$ changes over a range $2g$. For other parameters, i.e., $0 < |\delta| < 1$, the energy spectrum ε_k, which lies in the range $[2g|\delta|, 2g]$, shrinks as $|\delta|$ approaches unity. There is an energy gap between the two subbands $4g|\delta|$.

Previously, a Möbius strip [28,30,31] was proposed to fabricate novel devices and materials [32], e.g., topological insulators and negative-index metamaterials [33,35]. Although it seems that the ring with a Möbius boundary condition in this paper is somewhat different from the Möbius strip in Refs. [31,33,35], we remark that the ring with a Möbius boundary condition can be considered as a Möbius strip in Hilbert space. A further comparison shows that the ring with a Möbius boundary condition is not evenly twisted as the

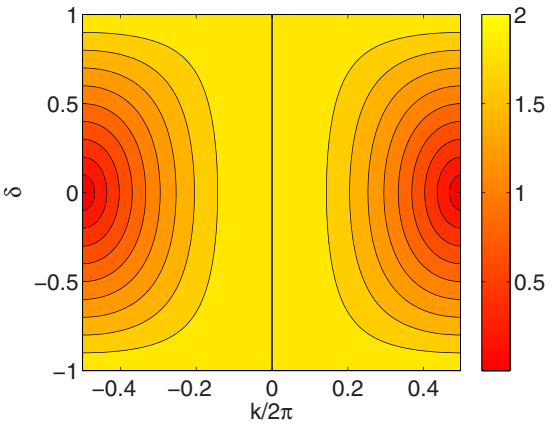

FIG. 2. Energy spectrum ε_k of A_k modes vs dimerization δ with $N = 800$, and $g/\xi = 1$, and $\xi = 10$ ps^{-1}. For any given δ, ε_k varies in the range $[2g|\delta|,2g]$.

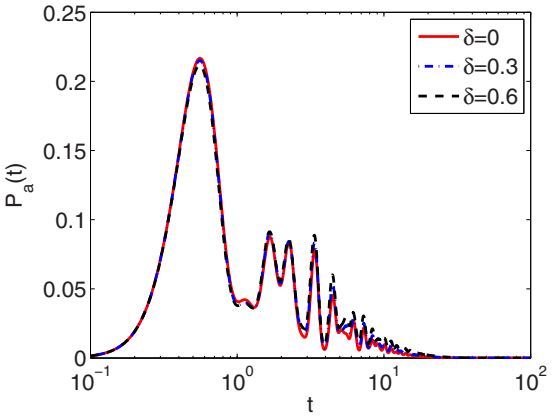

FIG. 3. Population dynamics of acceptor $P_a(t) = |\alpha_A|^2$ with a Möbius ring for $\delta = 0$ (red solid line), $\delta = 0.3$ (blue dashed-dotted line), and $\delta = 0.6$ (black dashed line). Other parameters are $N = 8$, $\omega/\xi = \varepsilon_A/\xi = -6$, $J/\xi = 1$, $g/\xi = 1$, $\Gamma/\xi = 0.3$, and $\kappa/\Gamma = 1$ with $\xi = 10$ ps^{-1}.

previous Möbius strip. As a result of the Möbius boundary condition, the photon and acceptor are coupled to all the collective modes in the ring, and thus it leads to different quantum dynamics as compared to that for a ring with a periodical boundary condition.

III. NUMERICAL RESULTS

In this section, we consider the quantum dynamics of light harvesting by a Peierls distorted chain with a Möbius boundary condition. For an initial state $|\psi(0)\rangle = |1_b\rangle \equiv |1_b,0_A,0_{Ak},0_{Bk}\rangle$, the state of the total system at any time t,

$$|\psi(t)\rangle = \alpha_b|1_b\rangle + \alpha_A|1_A\rangle + \sum_k \beta_{Ak}|1_{Ak}\rangle + \sum_k \beta_{Bk}|1_{Bk}\rangle, \tag{12}$$

with $|1_A\rangle \equiv |0_b,1_A,0_{Ak},0_{Bk}\rangle$, $|1_{Ak}\rangle \equiv |0_b,0_A,1_{Ak},0_{Bk}\rangle$, $|1_{Bk}\rangle \equiv |0_b,0_A,0_{Ak},1_{Bk}\rangle$, is governed by the Schrödinger equation

$$i\partial_t|\psi(t)\rangle = H|\psi(t)\rangle, \tag{13}$$

if the system does not interact with the environment. However, an open quantum system inevitably suffers from decoherence due to the couplings to the environment. Generally speaking, the quantum dynamics in the presence of decoherence is described by the master equation instead of the Schrödinger equation. Despite this, it has been shown that the quantum dynamics for light harvesting can be well simulated by the quantum jump approach with a non-Hermitian Hamiltonian where the imaginary parts in the diagonal terms represent the decoherence processes [25,38]. In this case, the Hamiltonian H in Eq. (3) is obtained by replacing the energies of the acceptor and collective-excitation modes in the following way, i.e.,

$$A : \varepsilon_A \to \varepsilon'_A = \varepsilon_A - i\Gamma, \tag{14a}$$

$$A_k : \varepsilon_k \to \varepsilon_k^- = \varepsilon_k - i\kappa, \tag{14b}$$

$$B_k : -\varepsilon_k \to -\varepsilon_k^+ = -(\varepsilon_k + i\kappa), \tag{14c}$$

where κ and Γ are respectively the fluorescence rate at the donors and the charge-separation rate at the acceptor.

It was shown [21] that in a composite system including a photon, and an acceptor, and a perfect ring with a periodical boundary condition, the quantum dynamics of the total system can be effectively modeled as the interaction of the photon and acceptor with the donor's single collective-excitation mode. Furthermore, as proven in Appendix B, both the photon and acceptor are still coupled to the same collective mode of the donor ring even when the ring is dimerized. However, the situation is different when we explore coherent energy transfer in a dimerized Möbius ring.

In Fig. 3, we plot the population of acceptor $P_a(t) = |\alpha_A(t)|^2$ versus time for $\delta = 0$. The population quickly rises to a maximum and then it is followed by damped oscillations. In Ref. [21], it was shown that the population dynamics oscillates with a unique frequency, which corresponds to the eigenenergy of the dark state. Here, the frequency with which $P_a(t)$ oscillates clearly depends on the time, and there is collapse-and-revival-like phenomenon. These observations indicate that the acceptor in our model is obviously coupled to multimodes, which will be further explored by the coupling constants later. In order to investigate the dimerization's effect, we also plot the population dynamics for a finite δ, e.g., $\delta = 0.3$ and $\delta = 0.6$. Clearly, the quantum dynamics in a Möbius ring is subtly influenced by the dimerization. For a finite δ, the vibration frequency is slightly modified by increasing δ, since the width of the donor bands shrinks, as shown in Fig. 2. Notice that for a finite δ the population is larger than that for $\delta = 0$ at all times. This implies that the transfer efficiency might be larger for a finite δ, as the efficiency is the integral of the acceptor's population versus time [cf. Eq. (15)].

To quantitatively characterize the energy transfer, there is the transfer efficiency η defined as [39–41]

$$\eta = 2\Gamma \int_0^\infty |\alpha_A(t)|^2 dt. \tag{15}$$

In Fig. 4, we investigate the dependence of transfer efficiency on the dimerization δ and the detuning $\Delta = \omega - \varepsilon_A$. For an evenly distributed donor ring, i.e., $\delta = 0$, the transfer efficiency reaches maximum near the resonance, i.e., $\Delta = 0$, which is

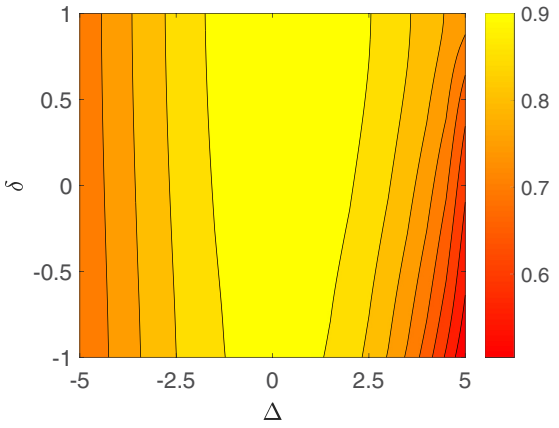

FIG. 4. Transfer efficiency η vs dimerization δ and detuning $\Delta = \omega - \varepsilon_A$. Other parameters are $N = 8$, $\omega/\xi = \varepsilon_A/\xi = -6$, $J/\xi = 1$, $g/\xi = 1$, $\Gamma/\xi = 0.3$, and $\kappa/\Gamma = 1$ with $\xi = 10$ ps^{-1}.

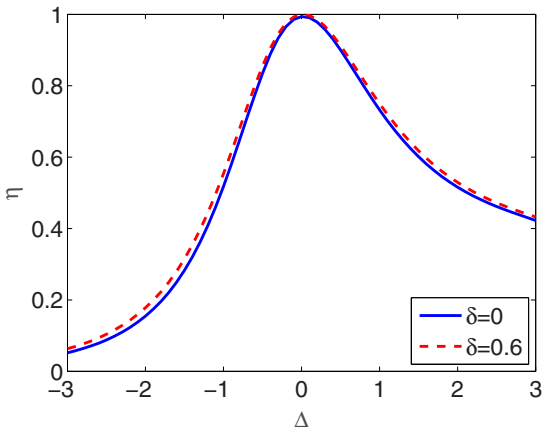

FIG. 5. Transfer efficiency η vs detuning $\Delta = \omega - \varepsilon_A$ by the perturbation theory. The parameters are the same as in Fig. 4.

slightly different from that discovered in Ref. [21]. As the photon frequency deviates from the resonance, the transfer efficiency quickly drops. When we further investigate the case for a dimerized ring with $\delta > 0$, the transfer efficiency has been increased in the whole frequency domain. Namely, the frequency domain for the high efficiency has been broadened. For negative detuning, the difference between an equally spaced ring and a dimerized ring is so small that the contour is almost parallel to the vertical axis. When the photon frequency is increased towards the donor band, the dimerized ring becomes more and more efficient than the equally spaced ring. In this case with an equally spaced ring, more dissipative modes in the lower B_k subband have been probed because the energy band is wider and the couplings h_{Bk} are stronger [cf. Figs. 2 and 6(b)]. In other words, although the collective modes in the donor ring are lossy, the photon explores the virtual excitation in the donor ring to avoid energy loss and delivers the energy to the reaction center. Noticeably, for $\delta < 0$, the dimerized ring becomes less efficient than the equally spaced ring as the frequency domain for the high efficiency shrinks. We remark that this and the asymmetry with respect to $\Delta = 0$ may be attributed to the chiral characteristics of the Möbius ring.

To validate the above numerical simulation, we also calculate the quantum dynamics and light-harvesting efficiency by the perturbation theory. The details are presented in Appendix C. In Ref. [42], it has been proven that the Wigner-Weisskopf approximation is equivalent to the perturbation theory in the study of an excited state coupled to a continuum. Here, we generalize the perturbation theory to the investigation of coherent energy transfer between few bodies via a continuum. In Fig. 5, the energy transfer efficiency of a dimerized ring is generally larger than that of an equally spaced ring. In the negative-detuning regime, the difference between the two rings by the perturbation theory is larger than that by the exact numerical simulation. That might be attributed to the higher-order correction. This result is qualitatively consistent with Fig. 4.

In order to explore the underlying physical mechanism, we turn to the coupling constants $|h_{Ak}|$ and $|h_{Bk}|$, as shown in Fig. 6. For $\delta = 0$, there is a sharp peak around $k = 0$ for both $|h_{Ak}|$ and $|h_{Bk}|$. This is significantly different from the case in Ref. [21]. Therein, both the photon and acceptor are only coupled to a single collective mode in the donor ring. It effectively forms a Λ-type configuration, and thus can explore the dark state to facilitate the energy transfer. Furthermore, we also plot $|h_{Ak}|$ and $|h_{Bk}|$ for $\delta = 0.6$. Although the coupling constant $|h_{Ak}|$ for $\delta = 0.6$ almost coincides with the ones for $\delta = 0$, the coupling constants $|h_{Bk}|$ are significantly suppressed when dimerization occurs. In addition, because $|h_{Bk}|$ are generally smaller than $|h_{Ak}|$ by an order, the transfer efficiency is slightly tuned by the dimerization.

IV. PHYSICAL REALIZATION

In the above sections, we explored coherent energy transfer in a dimerized ring with a Möbius boundary condition. Since this kind of molecule has yet to be discovered in natural photosynthetic complexes, in this section we will discuss its possible realization in experiment.

In Ref. [43], artificial light-harvesting systems are experimentally fabricated by zinc-phthalocyanine molecules. By using a scanning tunneling microscope, different configurations of artificial light harvesting are realized by engineering the intermolecular distances and relative orientations of molecular electric dipoles. The intermolecular dipole-dipole couplings are visualized by scanning tunneling microscope-induced luminescence. Here, inspired by these breakthroughs, we propose realizing a dimerized ring with a Möbius boundary condition for artificial light harvesting.

As shown in Fig. 7, the molecules are sequentially arranged in a circle with radius R and angular coordinate being $\alpha_i = 2\pi i/N$ $(i = 1,2,\ldots,N)$. The dipole-dipole coupling between two molecules separated by $\vec{r}_{ij}$ is

$$g_{ij} = \frac{\vec{\mu}_i \cdot \vec{\mu}_j}{4\pi\varepsilon_0 r_{ij}^3} - \frac{3(\vec{\mu}_i \cdot \vec{r}_{ij})(\vec{\mu}_j \cdot \vec{r}_{ij})}{4\pi\varepsilon_0 r_{ij}^5}, \tag{16}$$

where $\vec{\mu}_i$ is the electric dipole of molecule i, and ε_0 is the permittivity of vacuum.

The molecular dipole i is aligned in the D_i-O-z plane. The last molecular dipole is perpendicular to the circle. The ith

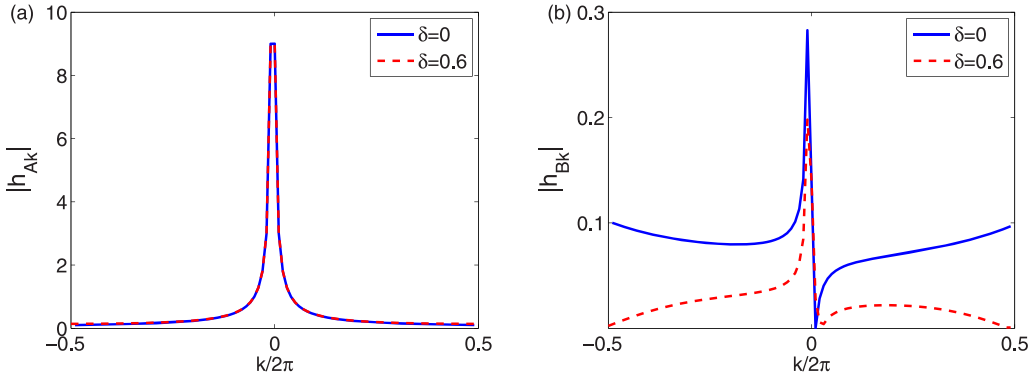

FIG. 6. Coupling constants (a) $|h_{Ak}|$ and (b) $|h_{Bk}|$ vs momentum k for dimerization $\delta = 0$ (blue solid line) and $\delta = 0.6$ (red dashed line). Other parameters are $N = 200$ and $g/\xi = 1$.

molecular dipole is rotated by an angle θ_i from the z axis, which is listed in Table I. Notice that $\vec{\mu}_1$ is not exactly antiparallel to $\vec{\mu}_8$ because $\vec{r}_{81}$ is not perpendicular to either $\vec{\mu}_1$ or $\vec{\mu}_8$, and this results in a nonvanishing second term on the right-hand side of Eq. (16). In this way, $g_{i,i+1} = -g_{81} = 8.725R^{-3}$ a.u. $(i = 1,2,\ldots,7)$ and thus the Möbius boundary condition is realized since the Nth molecular dipole is antiparallel to the first molecular dipole. As demonstrated above, an equally spaced Möbius ring is proposed by appropriately arranging the molecular positions in the ring and their dipolar orientations. In the same way, a Möbius ring with dimerization can be realized as the number of parameters $(\alpha_i,\theta_i,\phi_i)$ is more than the number of constraints $g_{i,i+1} = -g_{N1}$ $(i = 1,2,\ldots,7)$. We further remark that because the dipole-dipole interaction is inversely proportional to r_{ij}^3, the distance between two next-nearest neighbors is almost twice the distance between two nearest neighbors and thus the next-nearest-neighboring coupling $g_{i,i+2} = g_{i,i+1}/8$ can be omitted. In conclusion, the dimerized Möbius ring for photosynthetic energy transfer is configured.

V. DISCUSSION AND CONCLUSION

In this paper, we investigate the quantum dynamics of light harvesting in a Peierls distorted ring with a Möbius boundary condition. Due to the nontrivial Möbius topology, there are two energy bands for the excitation in the ring when the donors in the ring are dimerized. Because both the photon and acceptor interact with all collective-excitation modes in the Möbius ring, the quantum dynamics and thus the efficiency for light harvesting are effectively influenced by the presence of dimerization. By numerical simulations, we show that when the donors in the Möbius ring are dimerized, the energy transfer is generally optimal for a wide range of photon frequencies. In order to suppress the fluorescence, the photon utilizes the virtual excitation in the donor ring to efficiently transfer energy to the reaction center. Besides, the dimerized Möbius ring is also robust against moderate static disorders. Our discoveries, together with the previous findings [12,18,20,21,26,44], may be beneficial for the future design of optimal artificial light harvesting.

In this paper, we have not taken the effects of temperature into consideration. In Ref. [45], it has been shown that the thermal effects would lead to increased dephasing rates and thus might dynamically localize the wave function on the LH2 ring. In Eq. (14), both the fluorescence rate κ and charge-separation rate Γ, which play a subtle role in energy transfer, increase monotonically along with the rise in temperature. As implied by the quantum jump approach [25], the fluorescence leads to a harmful energy loss, while charge separation traps the energy which will be utilized in subsequent useful chemical reactions. When the temperature is sufficiently low, the fluorescence and charge-separation rates might be slow. Under this circumstance, coherent evolution dominates in the quantum dynamics. Thus, although the captured photon energy will be coherently vibrating between the donors and the acceptor, it cannot be effectively trapped by the acceptor. As the temperature rises, the charge-separation rate increases faster than the fluorescence rate, and thus the charge separation is superior to fluorescence decay. Also, the coherently transferred population at the acceptor will be trapped because the enlarged charge-separation rate prevents the population at

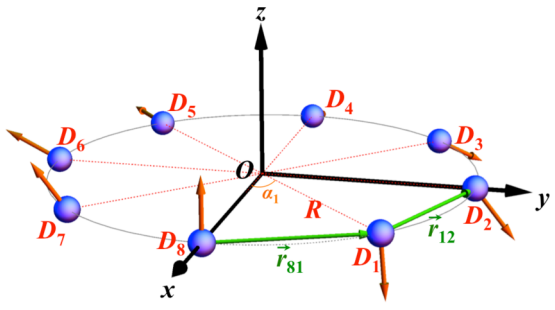

FIG. 7. Physical realization of a ring with a Möbius boundary condition. The zinc-phthalocyanine molecules are equally spaced in the circle with radius R. The ith molecular dipole is aligned in the D_i-O-z plane, and it is rotated by an angle θ_i from the z axis.

TABLE I. The orientations of molecular electric dipoles: $\vec{\mu}_i \parallel \sin\theta_i(\cos\phi_i\vec{e}_x + \sin\phi_i\vec{e}_y) + \cos\phi_i\vec{e}_z$ with $\phi_i = 2\pi i/N$. The eighth dipole is parallel to the z axis, i.e., $\theta_8 = 0$.

i	1	2	3	4	5	6	7
θ_i/π	0.9538	0.7867	0.6601	0.5714	0.4828	0.3561	0.1891

the acceptor from being back-transferred. If the temperature increases further, the fluorescence rate at the donor sites will be sufficiently large. In this case, the population transferred to the donors will be dynamically localized by fluorescence decay. In brief, we expect an optimal temperature which can facilitate energy transfer.

In practice, a change in (protein) environment inevitably leads to static and dynamic disorders in the transition energies of chlorophylls in natural photosynthesis [22,46,47]. In Ref. [21], assuming that all site energies of the donors are homogeneous, the absorbed photon energy utilizes a dark-state mechanism to effectively avoid fluorescence loss via the donors. However, this mechanism might not work well when static and dynamic disorders take place, as static disorder would probably modify the transfer dynamics and thus the parametric dependence [27,48]. By numerical simulations, which are not shown here, we can prove that for moderate static disorder, the energy transfer efficiency for a dimerized ring is superior to that for an equally spaced ring. This result demonstrates that our scheme to utilize a dimerized ring with a Möbius boundary condition is robust for small and moderate static disorders.

ACKNOWLEDGMENTS

We are thankful for stimulating discussions with C. P. Sun, H. Dong, and Y. N. Fang. This work is supported by NSFC (Grants No. 11505007 and No. 11534002), the National Basic Research Program of China (Grants No. 2016YFA0301201 and No. 2014CB921403), and the NSAF (Grants No. U1730449 and No. U1530401), and the Open Research Fund Program of the State Key Laboratory of Low-Dimensional Quantum Physics, Tsinghua University Grant No. KF201502.

APPENDIX A: DIAGONALIZATION OF MÖBIUS HAMILTONIAN

The dimerized ring with a Möbius boundary condition is described by

$$H_{\mathrm{PM}} = \sum_{j=1}^{N-1} g[1-(-1)^j\delta]d_{j+1}^\dagger d_j - g[1-(-1)^N\delta]d_1^\dagger d_N + \mathrm{H.c.}, \tag{A1}$$

where $|\delta| < 1$ is a dimensionless dimerization constant. By applying a unitary transformation

$$U = \sum_j e^{ij\frac{\pi}{N}} d_j^\dagger d_j, \tag{A2}$$

the Hamiltonian reads

$$UH_{\mathrm{PM}}U^\dagger = \sum_{j=1}^{N/2}[g_0(1-\delta)d_{2j+1}^\dagger d_{2j} + g_0(1+\delta)d_{2j}^\dagger d_{2j-1}] + \mathrm{H.c.}, \tag{A3}$$

where

$$g_0 = ge^{i\frac{\pi}{N}}. \tag{A4}$$

After a unitary transformation, the Möbius boundary condition has been canceled.

By defining fermion operators [49]

$$\alpha_k = \frac{1}{\sqrt{N}}\sum_{j=1}^{N/2} e^{-ikj}(d_{2j-1} + e^{i\theta_k}d_{2j}), \tag{A5a}$$

$$\beta_k = \frac{1}{\sqrt{N}}\sum_{j=1}^{N/2} e^{-ikj}(d_{2j-1} - e^{i\theta_k}d_{2j}), \tag{A5b}$$

where the momentum is

$$k = \frac{4\pi}{N}\left(0,1,2,\cdots\frac{N}{2}-1\right) - \pi + \frac{2\pi}{N}, \tag{A6}$$

$$e^{i\theta_k} = \frac{g}{\varepsilon_k}\left[(1+\delta)e^{-i\frac{\pi}{N}} + (1-\delta)e^{-i\left(k-\frac{\pi}{N}\right)}\right], \tag{A7}$$

$$\varepsilon_k = 2g\sqrt{\cos^2\left(\frac{k}{2}-\frac{\pi}{N}\right) + \delta^2\sin^2\left(\frac{k}{2}-\frac{\pi}{N}\right)} \tag{A8}$$

is the eigenenergy, N is an even number, and

$$UH_{\mathrm{PM}}U^\dagger = \sum_k \varepsilon_k(\alpha_k^\dagger\alpha_k - \beta_k^\dagger\beta_k). \tag{A9}$$

Here, the momentum is chosen in such a way that $\cos\left(\frac{k}{2}-\frac{\pi}{N}\right) \geqslant 0$ for $\delta = 0$ and thus the eigenenergies $\varepsilon_k = 2g\cos\left(\frac{k}{2}-\frac{\pi}{N}\right)$. Therefore, the original Hamiltonian can be diagonalized as

$$H_{\mathrm{PM}} = \sum_k \varepsilon_k(A_k^\dagger A_k - B_k^\dagger B_k), \tag{A10}$$

where the annihilation operators of the collective-excitation modes of the two bands $A_k = \alpha_k U$, $B_k = \beta_k U$ are

$$A_k = \sum_{j=1}^{N/2}\frac{e^{-ikj}}{\sqrt{N}}\left[e^{i(2j-1)\frac{\pi}{N}}d_{2j-1} + e^{i\left(\theta_k+2j\frac{\pi}{N}\right)}d_{2j}\right],$$

$$B_k = \sum_{j=1}^{N/2}\frac{e^{-ikj}}{\sqrt{N}}\left[e^{i(2j-1)\frac{\pi}{N}}d_{2j-1} - e^{i\left(\theta_k+2j\frac{\pi}{N}\right)}d_{2j}\right].$$

According to Eq. (A10), there are two subbands in the dimerized chain, i.e., ε_k and $-\varepsilon_k$. For the upper band, there is a minimum $2|g\delta|$ at $k = \pi + \frac{2\pi}{N}$, while for the lower band, there is a maximum $-2|g\delta|$ also at $k = \pi + \frac{2\pi}{N}$. Therefore, there is an energy gap between the two subbands $4|g\delta|$ as long as the ring is dimerized.

APPENDIX B: LIGHT HARVESTING BY A RING WITH A PERIODICAL BOUNDARY CONDITION

The Hamiltonian for a dimerized ring with a periodical boundary condition reads

$$H = \omega b^\dagger b + \varepsilon_A A^\dagger A + \sum_j g[1-(-1)^j\delta]d_j^\dagger d_{j+1} + \sum_j(Jd_j^\dagger b + \xi d_j^\dagger A) + \mathrm{H.c.} \tag{B1}$$

We define two sets of collective-excitation operators,

$$\alpha_k = \frac{1}{\sqrt{N}} \sum_{j=1}^{N/2} e^{-ikj}(d_{2j-1} - e^{i\theta_k} d_{2j}), \tag{B2a}$$

$$\beta_k = \frac{1}{\sqrt{N}} \sum_{j=1}^{N/2} e^{-ikj}(d_{2j-1} + e^{i\theta_k} d_{2j}), \tag{B2b}$$

where $k = 4\pi(n-1)/N$, $n = 1,2,\ldots,N/2$, and

$$e^{i\theta_k} = [(1+\delta) + (1-\delta)e^{-ik}]g/\varepsilon_k, \tag{B3}$$

$$\varepsilon_k = 2g\sqrt{\cos^2(k/2) + \delta^2 \sin^2(k/2)}. \tag{B4}$$

Thus, the Hamiltonian is transformed as

$$H = \omega b^\dagger b + \varepsilon_A A^\dagger A + \sum_k \varepsilon_k(\beta_k^\dagger \beta_k - \alpha_k^\dagger \alpha_k) + \sqrt{N}\beta_0^\dagger(Jb + \xi A) + \text{H.c.} \tag{B5}$$

Since only the zero-momentum mode

$$\beta_0 = \frac{1}{\sqrt{N}} \sum_{j=1}^{N} d_j \tag{B6}$$

with eigenenergy $\varepsilon_0 = 2g$ is coupled to the photon and acceptor, the effective Hamiltonian is further simplified as

$$H_{\text{eff}} = \omega b^\dagger b + 2g\beta_0^\dagger \beta_0 + \varepsilon_A A^\dagger A + \sqrt{N}\beta_0^\dagger(Jb + \xi A) + \text{H.c.}$$

In conclusion, for a ring with a periodical boundary condition, both the photon and acceptor are coupled to the same collective-excitation mode irrespective of the dimerization in the ring. In other words, we have proven that the quantum dynamics of light harvesting by a ring with a periodical boundary condition is not affected by the dimerization.

APPENDIX C: EQUIVALENCE OF PRESENT THEORY AND WIGNER-WEISSKOPF APPROXIMATION

The quantum dynamics in light harvesting is governed by the Schrödinger equation, which is equivalent to a set of coupled differential equations. Formally, it can be solved by a Laplace transformation. However, due to the presence of a branch cut, the exact solution may not be easily obtained. Generally speaking, it can be solved by the Wigner-Weisskopf approximation [50–52]. In Ref. [42], it has been proven that the Wigner-Weisskopf approximation is equivalent to the perturbation theory in the study of an excited state of a few-body system coupled to a continuum. Therefore, we make use of the perturbation theory to investigate the quantum dynamics of light harvesting in a dimerized Möbius chain.

For an initial state $|\psi(0)\rangle = |1_b\rangle$, the state of a system at any time t,

$$|\psi(t)\rangle = \alpha_b|1_b\rangle + \alpha_A|1_A\rangle + \sum_k(\beta_{Ak}|1_{Ak}\rangle + \beta_{Bk}|1_{Bk}\rangle),$$

is governed by Schrödinger equation $i\partial_t|\psi(t)\rangle = H|\psi(t)\rangle$.

We obtain a set of equations for the coefficients,

$$i\dot{\alpha}_b = \omega\alpha_b + \epsilon\sum_k J_{Ak}^*\beta_{Ak} + \epsilon\sum_k J_{Bk}^*\beta_{Bk}, \tag{C1a}$$

$$i\dot{\alpha}_A = \varepsilon_A'\alpha_A + \epsilon\sum_k \xi_{Ak}^*\beta_{Ak} + \epsilon\sum_k \xi_{Bk}^*\beta_{Bk}, \tag{C1b}$$

$$i\dot{\beta}_{Ak} = \varepsilon_k^-\beta_{Ak} + \epsilon\xi_{Ak}\alpha_A + \epsilon J_{Ak}\alpha_b, \tag{C1c}$$

$$i\dot{\beta}_{Bk} = -\varepsilon_k^+\beta_{Bk} + \epsilon\xi_{Bk}\alpha_A + \epsilon J_{Bk}\alpha_b, \tag{C1d}$$

where the parameter ϵ is introduced to keep track of the orders of perturbation.

By introducing renormalized frequencies

$$\Omega_b = \omega + \epsilon\Omega_b^{(1)} + \epsilon^2\Omega_b^{(2)} + \epsilon^3\Omega_b^{(3)} + \cdots, \tag{C2a}$$

$$\Omega_A = \varepsilon_A' + \epsilon\Omega_A^{(1)} + \epsilon^2\Omega_A^{(2)} + \epsilon^3\Omega_A^{(3)} + \cdots, \tag{C2b}$$

$$\Omega_{Ak} = \varepsilon_k^- + \epsilon\Omega_{Ak}^{(1)} + \epsilon^2\Omega_{Ak}^{(2)} + \epsilon^3\Omega_{Ak}^{(3)} + \cdots, \tag{C2c}$$

$$\Omega_{Bk} = -\varepsilon_k^+ + \epsilon\Omega_{Bk}^{(1)} + \epsilon^2\Omega_{Bk}^{(2)} + \epsilon^3\Omega_{Bk}^{(3)} + \cdots, \tag{C2d}$$

defining dimensionless times

$$\tau_b = \Omega_b t, \quad \tau_A = \Omega_A t, \quad \tau_{Ak} = \Omega_{Ak} t, \quad \tau_{Bk} = \Omega_{Bk} t, \tag{C3}$$

and expanding the coefficients as

$$\alpha_b = \alpha_b^{(0)} + \epsilon\alpha_b^{(1)} + \epsilon^2\alpha_b^{(2)} + \epsilon^3\alpha_b^{(3)} + \cdots, \tag{C4a}$$

$$\alpha_A = \alpha_A^{(0)} + \epsilon\alpha_A^{(1)} + \epsilon^2\alpha_A^{(2)} + \epsilon^3\alpha_A^{(3)} + \cdots, \tag{C4b}$$

$$\beta_{Ak} = \beta_{Ak}^{(0)} + \epsilon\beta_{Ak}^{(1)} + \epsilon^2\beta_{Ak}^{(2)} + \epsilon^3\beta_{Ak}^{(3)} + \cdots, \tag{C4c}$$

$$\beta_{Bk} = \beta_{Bk}^{(0)} + \epsilon\beta_{Bk}^{(1)} + \epsilon^2\beta_{Bk}^{(2)} + \epsilon^3\beta_{Bk}^{(3)} + \cdots, \tag{C4d}$$

we could reexpress the Schrödinger equation and obtain different order equations. In Eqs. (C2) and (C4), the superscripts label the order.

By comparing the coefficients of the same order on both sides, we could obtain, to the order of ϵ^2, the probability amplitudes as

$$\alpha_b(t) = A_b e^{-i\tau_b} + \sum_k\left(\frac{B_{Ak}J_{Ak}^*}{\varepsilon_k^- - \omega}e^{-i\tau_{Ak}} + \frac{B_{Bk}J_{Bk}^*}{-\varepsilon_k^+ - \omega}e^{-i\tau_{Bk}}\right),$$

$$\alpha_A(t) = A_A e^{-i\tau_A} + \sum_k\left(\frac{B_{Ak}\xi_{Ak}^*}{\varepsilon_k^- - \varepsilon_A'}e^{-i\tau_{Ak}} + \frac{B_{Bk}\xi_{Bk}^*}{-\varepsilon_k^+ - \varepsilon_A'}e^{-i\tau_{Bk}}\right) + A_b\frac{e^{-i\tau_b}}{\omega - \varepsilon_A'}\sum_k\left(\frac{J_{Ak}\xi_{Ak}^*}{\omega - \varepsilon_k^-} + \frac{J_{Bk}\xi_{Bk}^*}{\omega + \varepsilon_k^+}\right),$$

$$\beta_{Ak}(t) = B_{Ak}e^{-i\tau_{Ak}} + A_b\frac{J_{Ak}}{\omega - \varepsilon_k^-}e^{-i\tau_b},$$

$$\beta_{Bk}(t) = B_{Bk}e^{-i\tau_{Bk}} + A_b\frac{J_{Bk}}{\omega + \varepsilon_k^+}e^{-i\tau_b},$$

where we have used the initial condition, $\alpha_b(0) = 1$, $\alpha_A(0) = \beta_{Ak}(0) = \beta_{Bk}(0) = 0$, to obtain the coefficients

$$A_b = 1 - \sum_k\left[\frac{|J_{Ak}|^2}{(\omega - \varepsilon_k^-)^2} + \frac{|J_{Bk}|^2}{(\omega + \varepsilon_k^+)^2}\right],$$

$$A_A = -\sum_k \left[\frac{J_{Ak}}{(\omega-\varepsilon_k^-)}\frac{\xi_{Ak}^*}{(\varepsilon_A'-\varepsilon_k^-)}+\frac{J_{Bk}}{(\omega+\varepsilon_k^+)}\frac{\xi_{Bk}^*}{(\varepsilon_A'+\varepsilon_k^+)}\right] - \sum_k \left(\frac{J_{Ak}\xi_{Ak}^*}{\omega-\varepsilon_k^-}+\frac{J_{Bk}\xi_{Bk}^*}{\omega+\varepsilon_k^+}\right)\frac{1}{\omega-\varepsilon_A'},$$

$$B_{Ak} = -\frac{J_{Ak}}{\omega-\varepsilon_k^-},$$

$$B_{Bk} = -\frac{J_{Bk}}{\omega+\varepsilon_k^+}.$$

To the lowest order of ϵ, regardless of the fluorescence in the donor ring, and assuming there is a small imaginary part in ω, we recover the result under the Wigner-Weisskopf approximation as

$$\alpha_b(t) = \exp[-i(\omega+\Delta')t-\gamma t], \tag{C6}$$

where

$$\Delta' = \sum_k \wp\left(\frac{|J_{Ak}|^2}{\omega-\varepsilon_k}+\frac{|J_{Bk}|^2}{\omega+\varepsilon_k}\right), \tag{C7a}$$

$$\gamma = \pi\sum_k [|J_{Ak}|^2\delta(\omega-\varepsilon_k)+|J_{Bk}|^2\delta(\omega+\varepsilon_k)]. \tag{C7b}$$

[1] R. E. Blankenship, *Molecular Mechanisms of Photosynthesis* (Blackwell Science, Oxford, UK, 2002).

[2] V. May and O. Kühn, *Charge and Energy Transfer Dynamics in Molecular Systems*, 2nd ed. (Wiley-VCH, Weinheim, 2004).

[3] H. van Amerongen, L. Valkunas, and R. van Grondelle, *Photosynthetic Excitons* (World Scientific, Singapore, 2000).

[4] G. R. Fleming and M. A. Ratner, Grand challenges in basic energy sciences, Phys. Today **61** (7), 28 (2008).

[5] G. S. Engel, T. R. Calhoun, E. L. Read, T.-K. Ahn, T. Mancal, Y.-C. Cheng, R. E. Blankenship, and G. R. Fleming, Evidence for wavelike energy transfer through quantum coherence in photosynthetic systems, Nature (London) **446**, 782 (2007).

[6] H. Lee, Y.-C. Cheng, and G. R. Fleming, Coherence dynamics in photosynthesis: Protein protection of excitonic coherence, Science **316**, 1462 (2007).

[7] E. Collini, C. Y. Wong, K. E. Wilk, P. M. G. Curmi, P. Brumer, and G. D. Scholes, Coherently wired light-harvesting in photosynthetic marine algae at ambient temperature, Nature (London) **463**, 644 (2010).

[8] R. Hildner, D. Brinks, J. B. Nieder, R. J. Cogdell, and N. F. van Hulst, Quantum coherent energy transfer over varying pathways in single light-harvesting complexes, Science **340**, 1448 (2013).

[9] A. Ishizaki and G. R. Fleming, Theoretical examination of quantum coherence in a photosynthetic system at physiological temperature, Proc. Natl. Acad. Sci. USA **106**, 17255 (2009).

[10] Y.-C. Cheng and R. J. Silbey, Coherence in the B800 Ring of Purple Bacteria LH2, Phys. Rev. Lett. **96**, 028103 (2006).

[11] A. W. Chin, J. Prior, R. Rosenbach, F. Caycedo-Soler, S. F. Huelga, and M. B. Plenio, The role of non-equilibrium vibrational structures in electronic coherence and recoherence in pigment-protein complexes, Nat. Phys. **9**, 113 (2013).

[12] Q. Ai, T.-C. Yen, B.-Y. Jin, and Y.-C. Cheng, Clustered geometries exploiting quantum coherence effects for efficient energy transfer in light harvesting, J. Phys. Chem. Lett. **4**, 2577 (2013).

[13] M. Sarovar, A. Ishizaki, G. R. Fleming, and K. B. Whaley, Quantum entanglement in photosynthetic light harvesting complexes, Nat. Phys. **6**, 462 (2010).

[14] J.-Q. Liao, J.-F. Huang, L.-M. Kuang, and C. P. Sun, Coherent excitation-energy transfer and quantum entanglement in a dimer, Phys. Rev. A **82**, 052109 (2010).

[15] M. Mohseni, P. Rebentrost, S. Lloyd, and A. Aspuru-Guzik, Environment-assisted quantum walks in photosynthetic energy transfer, J. Chem. Phys. **129**, 174106 (2008).

[16] M. Qin, H. Z. Shen, X. L. Zhao, and X. X. Yi, Dynamics and quantumness of excitation energy transfer through a complex quantum network, Phys. Rev. E **90**, 042140 (2014).

[17] M.-J. Tao, Q. Ai, F.-G. Deng, and Y.-C. Cheng, Proposal for probing energy transfer pathway by single-molecule pump-dump experiment, Sci. Rep. **6**, 27535 (2016).

[18] J. L. Wu, R. J. Silbey, and J. S. Cao, Generic Mechanism of Optimal Energy Transfer Efficiency: A Scaling Theory of the Mean First Passage Time in Exciton Systems, Phys. Rev. Lett. **110**, 200402 (2013).

[19] S. Hoyer, A. Ishizaki, and K. B. Whaley, Spatial propagation of excitonic coherence enables ratcheted energy transfer, Phys. Rev. E **86**, 041911 (2012).

[20] S. Yang, D. Z. Xu, Z. Song, and C. P. Sun, Dimerization-assisted energy transport in light-harvesting complexes, J. Chem. Phys. **132**, 234501 (2010).

[21] H. Dong, D. Z. Xu, J. F. Huang, and C. P. Sun, Coherent excitation transfer via the dark-state channel in a bionic system, Light: Sci. Appl. **1**, e2 (2012).

[22] M. Sarovar, Y.-C. Cheng, and K. B. Whaley, Environmental correlation effects on excitation energy transfer in photosynthetic light harvesting, Phys. Rev. E **83**, 011906 (2011).

[23] P. Nalbach, D. Braun, and M. Thorwart, Exciton transfer dynamics and quantumness of energy transfer in the Fenna-Matthews-Olson complex, Phys. Rev. E **84**, 041926 (2011).

[24] B.-X. Wang, M.-J. Tao, Q. Ai, T. Xin, N. Lambert, D. Ruan, Y.-C. Cheng, F. Nori, F.-G. Deng, and G.-L. Long, Quantum simulation of photosynthetic energy transfer, arXiv:1801.09475.

[25] A. Olaya-Castro, C. F. Lee, F. F. Olsen, and N. F. Johnson, Efficiency of energy transfer in a light-harvesting system under quantum coherence, Phys. Rev. B **78**, 085115 (2008).

[26] L. Cleary, H. Chen, C. Chuang, R. J. Silbey, and J. S. Cao, Optimal fold symmetry of LH2 rings on a photosynthetic membrane, Proc. Natl. Acad. Sci. USA **110**, 8537 (2013).

[27] Y. Y. Wang, J. Qiu, Y. Q. Chu, M. Zhang, J. M. Cai, Q. Ai, and F. G. Deng, Phys. Rev. A **97**, 042313 (2018).

[28] E. Heilbronner, Hückel molecular orbitals of Möbius-type conformations of annulenes, Tetrahedron Lett. **5**, 1923 (1964).

[29] D. Ajami, O. Oeckler, A. Simon, and R. Herges, Synthesis of a Möbius aromatic hydrocarbon, Nature (London) **426**, 819 (2003).

[30] T. Yoneda, Y. M. Sung, J. M. Lim, D. Kim, and A. Osuka, Pd^{II} complexes of [44]- and [46]decaphyrins: The largest Hückel

aromatic and antiaromatic, and Möbius aromatic macrocycles, Angew. Chem. **126**, 13385 (2014).

[31] N. Zhao, H. Dong, S. Yang, and C. P. Sun, Observable topological effects in molecular devices with Möbius topology, Phys. Rev. B **79**, 125440 (2009).

[32] V. Balzani, A. Credi, and M. Venturi, *Molecular Devices and Machines: Concepts and Perspectives for the Nanoworld* (Wiley-VCH, Weinheim, 2008).

[33] Z. L. Guo, Z. R. Gong, H. Dong, and C. P. Sun, Möbius graphene strip as a topological insulator, Phys. Rev. B **80**, 195310 (2009).

[34] C. W. Chang, M. Liu, S. Nam, S. Zhang, Y. Liu, G. Bartal, and X. Zhang, Optical Möbius Symmetry in Metamaterials, Phys. Rev. Lett. **105**, 235501 (2010).

[35] Y. N. Fang, Y. Shen, Q. Ai, and C. P. Sun, Negative refraction in Möbius molecules, Phys. Rev. A **94**, 043805 (2016).

[36] R. E. Peierls, *Quantum Theory of Solids* (Oxford University Press, London, 1955).

[37] Y. Shen and B.-Y. Jin, Correspondence between Gentile oscillators and N-annulenes, J. Phys. Chem. A **117**, 12540 (2013).

[38] Q. Ai, Y.-J. Fan, B.-Y. Jin, and Y.-C. Cheng, An efficient quantum jump method for coherent energy transfer dynamics in photosynthetic systems under the influence of laser fields, New J. Phys. **16**, 053033 (2014).

[39] F. Caruso, A. W. Chin, A. Datta, S. F. Huelga, and M. B. Plenio, Highly efficient energy excitation transfer in light-harvesting complexes: The fundamental role of noise-assisted transport, J. Chem. Phys. **131**, 105106 (2009).

[40] F. Fassioli and A. Olaya-Castro, Distribution of entanglement in light-harvesting complexes and their quantum efficiency, New J. Phys. **12**, 085006 (2010).

[41] B.-Q. Ai and S.-L. Zhu, Complex quantum network model of energy transfer in photosynthetic complexes, Phys. Rev. E **86**, 061917 (2012).

[42] Y. K. Wang and I. C. Khoo, On the Wigner-Weisskopf approximation in quantum optics, Opt. Commun. **11**, 323 (1974).

[43] Y. Zhang, Y. Luo, Y. Zhang, Y.-J. Yu, Y.-M. Kuang, L. Zhang, Q.-S. Meng, Y. Luo, J.-L. Yang, Z.-C. Dong, and J. G. Hou, Visualizing coherent intermolecular dipole-dipole coupling in real space, Nature (London) **531**, 623 (2016).

[44] M. del Rey, A. W. Chin, S. F. Huelga, and M. B. Plenio, Exploiting structured environments for efficient energy transfer: The phonon antenna mechanism, J. Phys. Chem. Lett. **4**, 903 (2013).

[45] J. M. Moix, Y. Zhao, and J. S. Cao, Equilibrium-reduced density matrix formulation: Influence of noise, disorder, and temperature on localization in excitonic systems, Phys. Rev. B **85**, 115412 (2012).

[46] H. Dong, S.-W. Li, Z. H. Yi, G. S. Agarwal, and M. O. Scully, Photon-blockade induced photon anti-bunching in photosynthetic Antennas with cyclic structures, arXiv:1608.04364.

[47] M. Pajusalu, R. Kunz, M. Ratsep, K. Timpmann, J. Kohler, and A. Freiberg, Unified analysis of ensemble and single-complex optical spectral data from light-harvesting complex-2 chromoproteins for gaining deeper insight into bacterial photosynthesis, Phys. Rev. E **92**, 052709 (2015).

[48] L. Cleary and J. S. Cao, Optimal thermal bath for robust excitation energy transfer in disordered light-harvesting complex 2 of purple bacteria, New J. Phys. **15**, 125030 (2013).

[49] M. X. Huo, Y. Li, Z. Song, and C. P. Sun, The Peierls distorted chain as a quantum data bus for quantum state transfer, Europhys. Lett. **84**, 30004 (2008).

[50] W. Weisskopf and E. Wigner, Calculation of the natural line width on the basis of Dirac's theory of light, Z. Phys. **63**, 54 (1930).

[51] P. L. Knight and L. Allen, The ladder approximation in quantum optics and the Wigner-Weisskopf theory, Phys. Lett. A **38**, 99 (1972).

[52] P. S. Lee, Y. C. Lee, and C. T. Chang, Multiple-time-scale analysis of spontaneous radiation processes. I. One- and two-particle systems, Phys. Rev. A **8**, 1722 (1973).